



Fermilab

PION PRODUCTION OF HEAVY  
QUARK MESON STATES DECAYING  
INTO  $\psi/J$  (3097)

OCT 5 1978

A Proposal Submitted By

R.G.Hicks, T.B.Kirk, R.Raja  
Fermilab  
Batavia, Illinois

J.Cooper, L.Holloway, L.Koester, U.Kruse, R.Sard, M.Shupe  
University of Illinois  
Urbana, Illinois

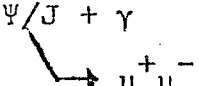
R.Milburn, W.Oliver, R.Thornton  
Tufts University  
Medford, Massachusetts

Spokesman:  
T.Kirk  
Fermilab  
Batavia, Illinois  
(312) 840-3683

51P99.

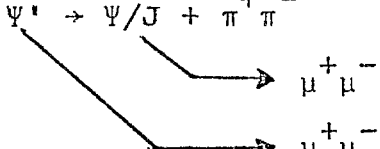
## Abstract

We propose to study the production of chi meson ( $\chi$ ) and psi-prime meson ( $\Psi'$ ) states with a beam of 225 GeV negative pions in the upgraded Chicago Cyclotron Magnet Spectrometer (CCM). The chi states will be detected via their decay to  $\Psi/J$ :

$$\chi \rightarrow \Psi/J + \gamma$$


The diagram shows a horizontal line representing the  $\chi$  meson. It splits into two branches: one going up and to the right to  $\Psi/J + \gamma$ , and another going down and to the right to  $\mu^+ \mu^-$ .

The psi-prime will be observed via its two pion decay to  $\Psi/J$ :

$$\Psi' \rightarrow \Psi/J + \pi^+ \pi^-$$


The diagram shows a horizontal line representing the  $\Psi'$  meson. It splits into two branches: one going up and to the right to  $\Psi/J + \pi^+ \pi^-$ , and another going down and to the right to  $\mu^+ \mu^-$ . The  $\pi^+ \pi^-$  branch further splits into two sub-branches, each leading to a  $\mu^+ \mu^-$  pair.

We have already observed the first reported pion production of  $\chi$  meson states<sup>1</sup>, but could not resolve the individual mass levels. We hope to increase the photon energy resolution by about a factor of five \*, and maintain the position resolution as it has been to enable us to resolve the individual chi states and increase the chi yields by a factor of 200 to gain information about the production rates and kinematic distributions. We hope to obtain a sample of 10,000  $\Psi/J$ 's and 3,000  $\chi$ 's in the proposed run.

A second goal of the experiment will be the production and detection of psi-prime with negative pions. We hope to produce a sample of about 500  $\Psi'$  events detected via the direct two muon decay and the cascade two pion decay to  $\Psi/J$ . A comparison of  $\Psi/J$  and  $\Psi'$  production rates, and the possible observation of new states above  $\Psi'$  which decay via photon emission into  $\Psi'$  will add more

---

\*Present energy resolution is limited by systematic errors in calibration.

information to the growing knowledge of heavy quark hadron processes.

To carry out the proposed program, we will need a total of  $3 \times 10^{12} \pi^-$  on target. This could be delivered in a period of about 10 weeks with either the Quadrupole Triplet or N30 Dichromatic Target Trains receiving about  $1.0 \times 10^{13}$ /burst.

Table of Contents

I.	Introduction	4
II.	Apparatus and Experimental Plan	7
III.	Trigger Rates and Event Yields	13
IV.	Personnel, Scheduling and Beam	18

Appendices

- A. Apparatus Acceptance for Dimuons and Trigger Rates
- B. The Pb Glass Array, Geometry and Resolution
- C. PDP11/45 Event Sampling Scheme for Dead Time Suppression
- D. Multi-Cell Threshold Cerenkov Counter Efficiency and Particle Separation Power
- E. Preprint:  $\pi^-$  Production of  $\psi$  and  $\chi$  Particles at 217 GeV/c

## I. Introduction

The physics of heavy (charmed) quarks has continued to be of intense interest since the discovery of  $\psi/J$  in 1974. In subsequent years, the study of bound heavy quark anti-quark pairs (charmonium) has proceeded rapidly with the discovery of higher  $J^P = 1^-$  states (psi family) and the establishment of  $J^P = 0^+, 1^+, 2^+$  states (chi family). The spectroscopy of states below the bare charm threshold is now fairly well established by experiments at SLAC and DESY storage rings and has been consolidated in the Particle Data Group Tables<sup>2</sup>.

The hadronic production mechanisms for charmed quarks on the other hand are rather unclear. To date, only the  $J^P = 1^-$  states (psi, upsilon) have been studied with any detail in hadronic processes<sup>3</sup>. These are the only quarkonium states that decay via the dilepton ( $\mu^+\mu^-$  or  $e^+e^-$ ) mode and are enormously easier to detect than states with  $J^P = 0^+, 1^+, 2^+$ , etc. (which cannot decay in this way).

From the hadronic production ratios of  $\psi/J$  and  $\psi'$  to one another and to the nonresonant dilepton background, it is clear that processes other than quark anti-quark annihilation (Drell-Yan process)<sup>4</sup> must be at work. One production mechanism that might account for the large psi family production above Drell-Yan background involves the production of chi particles followed by decay of the chi states to psi states with single photon emission. The initial chi's would be produced by the process of "gluon fusion" advanced by Carlson and Suaya<sup>5</sup> and by Ellis, Einhorn and Quigg<sup>6</sup>. If this process is dominant,

one might expect to see virtually all of the  $\psi/J$  particles produced in a strong interaction accompanied by a photon produced from the decay of a parent chi state.

To date only one paper has been published showing evidence for hadronic production (pp) of the chi mesons<sup>7</sup>. A previous effort by the present group has also detected the process; a clear  $\chi$  signal is seen in  $\pi^-p$  events with a  $\psi/J$  detected via  $\mu^+\mu^-$  decay plus one or more detected photons in the final state<sup>1</sup>. To date, these two experiments are the only ones which have detected hadronic production of the chi states at all! It is very interesting to observe, however, that the inferred fraction of  $\psi/J$ 's coming from a higher chi state is  $0.43 \pm 0.21$  for the pp and  $0.70 \pm 0.28$  for the  $\pi^-p$  experiments, respectively. The second result, especially, is very suggestive that the gluon fusion process<sup>5,6</sup> may be dominant.

The large  $\psi/J$  to  $\psi'$  production ratio for hadron collisions lends more support to the gluon fusion hypothesis<sup>5,8</sup>. If the branching ratios are divided out<sup>2</sup>, the relative production rates are about 15%,  $\psi'$  to  $\psi/J$ . We hope to see enough  $\psi'$  production in our open geometry to see if any of the  $\psi'$  comes from higher, as yet unknown, chi type states. This work is speculative but could be interesting. The method we propose to use to detect chi and psi production by negative pions is described in the following sections. If carried out in the way proposed, we will obtain a sample of about 10,000  $\psi/J$ 's in an open geometry. From this sample, we will reconstruct about 3,000  $\chi$  and perhaps 500  $\psi'$  events. With improvements in the lead glass,

the individual chi states will be resolved, resulting in helpful information on the proposed spin assignments and production mechanisms.

## II. Apparatus and Experiment Plan

We propose to use the rebuilt Chicago Cyclotron Spectrometer with a beam of  $10^7 \pi^-$  per burst at 225 GeV incident on a 4.5 cm beryllium metal target. The necessary beam can be produced either with the Quadrupole Triplet or N30 Dichromatic Trains in the Neutrino target tunnel and a targeted proton flux of about  $10^{13}$  protons per pulse. The apparatus is shown as it will be used in Figures 1a, b.

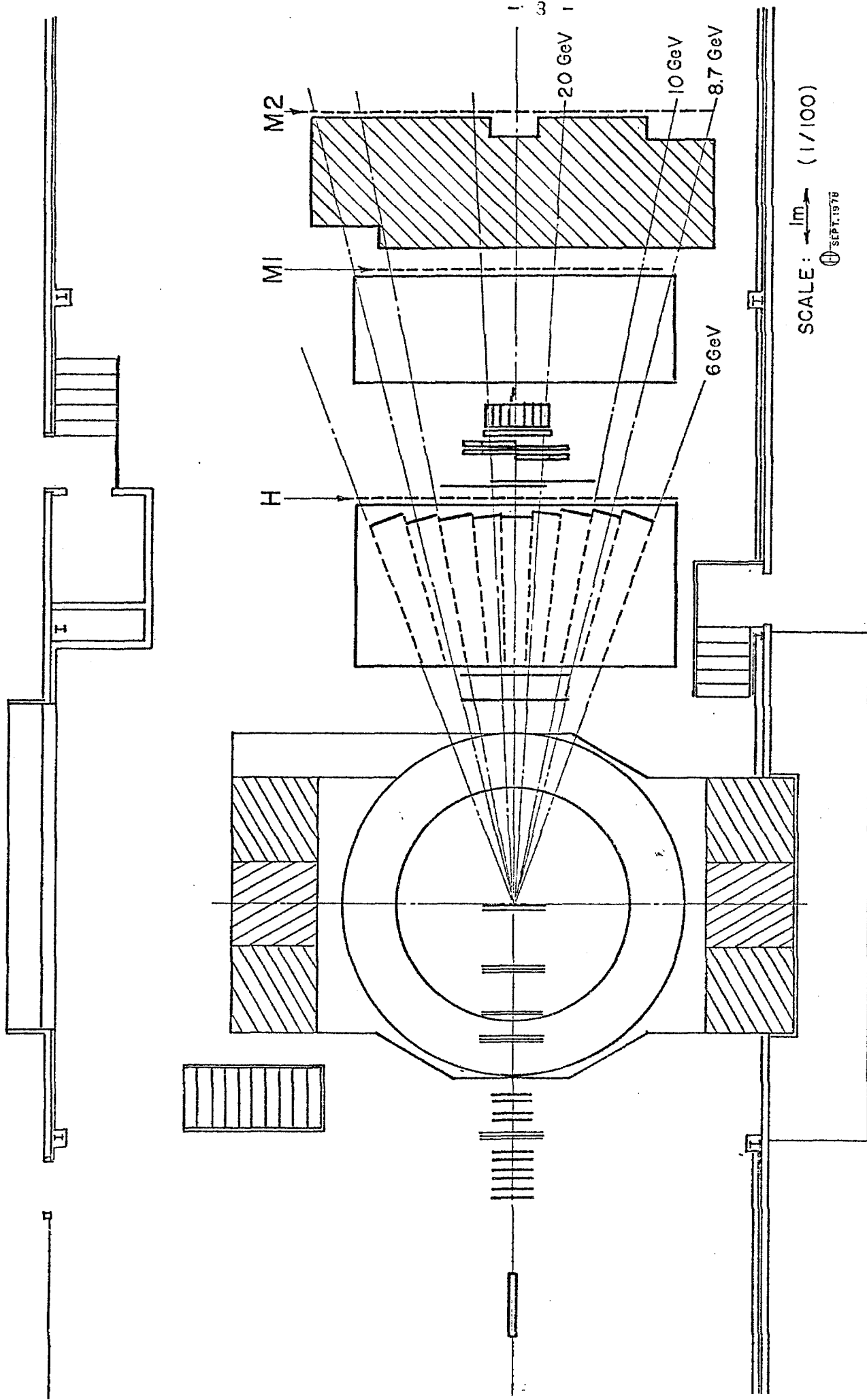
Beam particles pass through the existing momentum tagging/triggering system (T1-T6) in the N1 beam and enter a 4.5 cm Be target. Particles which are cleanly transported, have only one pion per r.f. bucket, are not accompanied by a halo muon and which interact in the target are candidates for event triggers.

The forward going particles from target interactions pass through a set of 10 MWPC planes of size 32" x 32" with 1/16" wire spacing into the CCM. Between the poles of the magnet are located a second set of 15 MWPC planes of size 1M x 1.2M with 2mm wire spacing and  $\pm 11.3^\circ$  stereo.

After passing through the magnet, neutral particles and charged particles with energies above about 7 GeV pass through a set of two 1.5M x 2.0M drift chambers, an 18 cell threshold Cerenkov counter, a second set of two drift chambers and into a large array of lead glass counters.

Photons from the event vertex shower in the Pb glass where their positions and energies are accurately measured. The proposed experiment will have a lead glass array which is larger





**MUON LAB**  
PLAN VIEW



in area than the E369 array by a factor of 3.5 and which will have an acceptance for chi related photons increased by a factor of 2.7. By carefully calibrating the individual blocks and continuously monitoring their gains, we will improve the energy resolution by a factor of nearly five over that reported in the attached preprint, thus providing for the separation of individual chi states. Details of the Pb glass array and its performance are given in Appendix B.

Muons from the decays of  $\psi/J$ ,  $\psi'$  and the much more copious background source of pion decays in flight pass through the steel absorber into the M counter array. Events in which two or more muons satisfy the M plane trigger conditions (see Appendix A) trigger the apparatus.

The PDP11/45 on-line computer will read in a small part of the data from CAMAC upon receipt of the event trigger. If a preliminary processing of the partial data sample by the PDP11 indicates the trigger is worth saving, the remaining data will be read into the computer. If not, the event will be aborted and the apparatus reset. In this way we hope to make a significant reduction in apparatus deadtime. In our former E369 run, the recharging time of the spark chambers was about 40 ms so read-in time was not the limiting consideration. The present apparatus has no such recharging limitation, and any gain that can be made in reducing read-in dead time is important. We believe that the average read-in time can be reduced from the old value of 40 ms to about 6 ms.

Good triggers will be stored during the beam spill on disk via a rotating core buffer system and re-written to magnetic tape between spills. If the software is available in time, we may attempt a second level of event editing as the triggers are read back in from disk and output to tape. This operation would save tape and some computer time but is not essential to the experiments proper functioning.

Each trigger will have hit coordinates from thirty-one MWPC planes, four two-dimensional drift chamber planes, nine hodoscopes, 108 lead glass blocks, eighteen Cerenkov cells, and miscellaneous pulse height, time-of-flight, blind scaler and other types of information. As a consequence, we will be able to reconstruct forward charged particle trajectories accurately and measure the position and energy of photons with precision sufficient to resolve the dominant  $\chi$  states. The  $\psi/J$  reconstructed mass will have a resolution comparable to or better than that achieved in E369 (about 100 MeV FWHM).

The existing pieces of the apparatus include the beam and tagging system, the target and its controls, the spectrometer magnet, the multi-cell Cerenkov counter, the scintillation counter arrays, the steel absorbers, the PDP11 computer and about 1/3 of the lead glass. The new equipment to be provided consists of multi-wire proportional chambers (Illinois/Fermilab), drift chambers (Fermilab), a new lead glass array (Illinois), and superconducting coils for the CCM (Fermilab). All of these items are underway, and prototypes of all the detectors exist and have been operated successfully. Additional steel absorber in front of the hadron filter (2M x 2M x 6M) will be needed for the dimuon trigger (Fermilab).

The superconducting coils for the CCM are being fabricated in the Meson Laboratory and will be finished in May 1979.

### III. Trigger Rates and Event Yields

We assume a beam of  $10^7 \pi^-$  in the N1 beamline with a 1.0 second flat top spill. Aside from the machine r.f. structure, we assume a duty factor of 0.85. From the raw flux  $B = 1.0 \times 10^7$ , we obtain a useful flux of  $8.8 \times 10^6$ /pulse after corrections for 2 particle buckets, accompanying halo muons and beam muons. We call this flux CB (clean beam):

$$B = T_1 \cdot T_2 \cdot T_3 \cdot T_4 \cdot T_5 \cdot T_6 \cdot \bar{V} = 1.0 \times 10^7 / \text{pulse}$$

$$CB = B \cdot \text{Prob}(\text{single } \pi / \text{bucket}) = 8.8 \times 10^6 \text{ pulse}^{-1}$$

This beam is incident on a target of 4.6 cm of beryllium, a target mass of  $8.5 \text{ gm/cm}^2$ . Trigger counters will add another 3 percent to make the target  $8.8 \text{ gm/cm}^2$ . We take the inelastic pion-proton cross section to be 21 mb. The inelastic rate in the target becomes:

$$I_{\pi p} = CB \cdot \text{Prob}(\text{interaction})$$

$$= (8.8 \times 10^6) (1 - e^{-t})$$

$$= (8.8 \times 10^6) (1 - e^{-0.11})$$

$$= 9.5 \times 10^5 \text{ pulse}^{-1}$$

$$\text{where; } t = \left( \frac{6.02 \times 10^{23}}{\text{gm}} \right) (21 \times 10^{-27} \text{ cm}^2) (8.8 \frac{\text{gm}}{\text{cm}^2}) = 0.11$$

From these interactions, we will trigger on a subset which has two muon hits in the M2 Hodoscope Plane. The details of the constraints placed on the M2 Plane counters and their exact geometry is discussed in Appendix A. Here we merely note that we have based our background calculations on a sample of real events taken from the exposure of the 30" Bubble Chamber to 147 GeV  $\pi^-$ 's/ The events are scaled to 225 GeV and all secondaries are treated like pions. Decays in flight producing muons are calculated by a Monte-Carlo technique and the resulting muons also

propagated. The quoted trigger rate results when muons from these decays in flight simulate the allowed M2 Plane trigger requirements. The majority of triggers come from this mundane background plus hadron punch-through and contribute  $45 \times 10^{-6}$  triggers per interacting pion.

In addition to the decay pions, there are real prompt muon pairs from sources like rho, phi, and omega  $\mu^+\mu^-$  decay, and finally from the process we seek, namely  $\psi/J$  and  $\psi'$  mesons. Table 1 summarizes these various  $2\mu$  rates.

Table 1  
Sources of  $2\mu$  Triggers  
( 4.5cm Be ;  $\sigma_{inel} = 21 \text{ mb}$ ;  $2\mu$  detected)

Source	Rate per Interacting Pion	
	'A' Geometry*	'B' Geometry
$\pi \rightarrow \mu$ decays +P.T.	$1.8 \times 10^{-5}$	$4.5 \times 10^{-5}$
low mass $\mu^+\mu^-$	$0.30 \times 10^{-5}$	$0.32 \times 10^{-5}$
$\psi/J \rightarrow \mu^+\mu^-$	$4.7 \times 10^{-8}$	$5.2 \times 10^{-8}$
$\psi' \rightarrow \mu^+\mu^-$	$7.0 \times 10^{-10}$	$8.3 \times 10^{-10}$
Total Rate	$2.1 \times 10^{-5}$	$4.8 \times 10^{-5}$
Measured Rate <sup>+</sup> in E369	$2.1 \times 10^{-5}$	

\*Geometry used in E369

<sup>+</sup>Normalized to equal target thickness with this proposal

Combining the trigger rate for the preferred 'B' Geometry with the inelastic CB interaction rate  $I_{\pi p}$  we get for the raw experiment trigger rate:

$$\begin{aligned}
 R_{\mu\mu} &= I_{\pi p} \cdot \text{Prob} (2\mu \text{ in MPlane Geometry}) \\
 &= (9.5 \times 10^5) (4.8 \times 10^{-5}) \\
 &= 46 \quad \text{pulse}^{-1}.
 \end{aligned}$$

$$\begin{aligned} R_{\psi J} &= I_{\pi p} \cdot \text{Rate } (\psi/J \rightarrow \mu^+ \mu^- \text{ detected}) \\ &= (9.5 \times 10^5) (5.2 \times 10^{-8}) \\ &= .049 \quad \text{pulse}^{-1}. \end{aligned}$$

$$\begin{aligned} R_{\psi'} &= I_{\pi p} \cdot \text{Rate } (\psi' \rightarrow \mu^+ \mu^-, \rightarrow \pi^+ \pi^- \psi/J \rightarrow \mu^+ \mu^- \text{ detected}) \\ &= (9.5 \times 10^5) (8 \times 10^{-10} + 17 \times 10^{-10}) \mu^+ \mu^- \\ &= .0025 \quad \text{pulse}^{-1}. \end{aligned}$$

To calculate the  $\psi/J$  and  $\psi'$  yields for the experiment, it is necessary to know the dead time fraction for the event trigger and the total beam delivered. As mentioned in the Introduction, we expect to get the average dead time per event down to 6 ms. Combined with the total  $2\mu$  trigger rate, this implies a live time fraction  $f_{\text{live}}$  of:

$$\begin{aligned} f_{\text{live}} &= \frac{1}{1 + R_{\mu\mu} \bar{\tau}_{\text{dead}}} \\ &= \frac{1}{1 + (45)(.006)} = .78 \end{aligned}$$

$$\text{where; } \bar{\tau}_{\text{dead}} = 6 \text{ ms}$$

Thus, the trigger and event yields become (for a 1.0 sec pulse):

$$\begin{aligned} T_{\mu\mu} &= R_{\mu\mu} \cdot f_{\text{live}} \\ &= (45)(.78) \\ &= 36 \quad \text{pulse}^{-1}, \text{ Total triggers per pulse} \end{aligned}$$

$$\begin{aligned} T_{\psi J} &= R_{\psi/J} \cdot f_{\text{live}} \\ &= (.049)(.78) \\ &= .038 \quad \text{pulse}^{-1}, \psi/J \text{ yield per pulse} \end{aligned}$$

$$\begin{aligned} T_{\psi'} &= R_{\psi'} \cdot f_{\text{live}} \\ &= (.0025)(.78) \\ &= .002 \quad \text{pulse}^{-1}, \psi' \text{ yield per pulse} \end{aligned}$$

We feel that it is necessary to obtain a sample of at least 10,000  $\psi/J$  to constitute a useful physics result. In order to



do this, we will need  $3 \times 10^5$  pulses of the machine at the design intensity of  $10^7$  per pulse. With an average pulse rate of 300 machine cycles per hour and 100 hours of useful beam per week, this represents a run of 10 weeks.

We now turn to a consideration of the chi yields which the above run will produce. We assume that we have 10,000  $\Psi/J$ 's and from our previous result that 70% of these come from chi states (Appendix E). The acceptance for detecting the chi decay photons has been determined by Monte Carlo (Appendix A) to be 47%. We, therefore, calculate the chi yield to be:

$$\begin{aligned} N_{\chi} &= N_{\Psi/J} \cdot f(\chi \rightarrow \Psi/J \gamma) \cdot E_{\gamma} \\ &= (10,000) (0.70) (0.47) \\ &= 3300 \quad \text{Total chi yield per experiment} \end{aligned}$$

These are enough to learn something about the relative populations of the three  $\chi$  states  $\chi(3555)$ ,  $\chi(3508)$  and  $\chi(3413)$ , and the kinematic distributions in Feynman  $x$  and  $P_{\perp}$ .

We summarize the yields for the experiment as Table 2:

Table 2  
Experimental Yields\*

Process	Total Events
$\pi^- p \rightarrow \psi/J + x$ $\downarrow$ $\mu^+ \mu^-$	10,000
$\pi^- p \rightarrow \psi' + x$ $\downarrow$ $\mu^+ \mu^-$	170
$\downarrow$ $\psi/J \pi^+ \pi^-$ $\downarrow$ $\mu^+ \mu^-$	330
$\pi^- p \rightarrow \chi + x$ $\downarrow$ $\psi/J + \gamma$ $\downarrow$ $\mu^+ \mu^-$	3300

\*Assumes  $3 \times 10^{12}$  pions incident on 4.5cm Be target with 'B' Geometry from Appendix A.

#### IV. Personnel, Scheduling and Beam

##### Strategy

The proposers of this experiment have completed a similar experiment, E-369, in the CCM Spectrometer during the period May-August 1977. The results of that experiment, in which pion production of  $\chi$  mesons was seen for the first time anywhere motivated the present proposal. The principal goal of E-369 was to produce bare charmed particles both with and without an accompanying  $\psi/J$ . The results to date on the bare charm search show only a hint of a D mass peak, but the chi region photons taken in conjunction with the  $\psi/J$  events give a clear signal. We are therefore inclined to pursue the chi production physics in preference to another run at bare charm.

##### CCM Spectrometer

Since the run of E-369, the CCM Spectrometer has been upgraded in a number of significant ways. Most important for the experiment proposed here is the elimination of all the magnetostrictive spark chambers with their long dead times and serious noise problems in favor of drift chambers now being constructed.

Of equal importance is the increase in solid angle subtended by lead glass counters. The E-369 array was small for the purposes of the chi production. We will now be able to subtend more solid angle by a factor 3.5 with a commensurate increase in detection efficiency for the chi meson states.

Addition of a new set of MWPC chambers in the CCM aperture will enable us to reconstruct low momentum tracks more precisely and with increased acceptance. This should help us in our search for  $\psi'$  production since the pions in the  $\pi^+\pi^-$  cascade to  $\psi/J$  will often have low laboratory energy (the  $\psi/J$  is biased by the apparatus acceptance to high  $X_F$ ).

Members of this proposal are actively involved in the CCM Spectrometer upgrade and are bringing the component parts to readiness at the present time. All the new apparatus should be ready for installation in the CCM before March 1, 1979. This schedule assumes that the superconducting magnet coils now being constructed in the Meson Detector Building will be installed on schedule in May 1979. A delay in the superconducting coil production would cause no harm; we would use the presently existing conventional coils and power supplies.

#### Lead Glass Array

The new lead glass will be assembled at Urbana during the Fall-Winter months. The lead glass has been ordered and will arrive by January 15, 1979. The new photo tubes and bases can be readied during November and December 1978. Necessary restacking and possible replacement of tube bases in the old lead glass array will be undertaken jointly by Tufts and Illinois and will likely happen in January or February.

#### MWPC Chambers

The new MWPC Chambers for the upstream part of the Spectrometer are already under construction at Fermilab and Illinois. One of five double plane chambers being constructed at Fermilab has already been tested in the E-448 run of Spring 1978. This chamber worked particularly well and had a measured efficiency in excess of 97%. The four remaining double planes of this group are nearing completion at Fermilab.

One of the five triple plane chambers designed by Illinois has been assembled and tested. It works as designed and has an efficiency above 95%. The remaining four modules are being assembled in Urbana.

### Cerenkov Counter

The multi-cell threshold Cerenkov counter used in E-369 will have its radiator path doubled to produce better counting efficiency. Although it sufficed to enrich the charged K content for tracks in the 8 to 30 GeV range in E-369, the low photo-electron yields will be increased to produce better K- $\pi$  discrimination by the added length of radiator (Appendix D). Otherwise, no changes are contemplated.

### Computer

A new data logging computer, a PDP-11/45 has been installed in the CCM Port-a-Kamp and the on-line data logging program is being constructed by Mr. Terry Lagerlund of the Fermilab Computer Department in consultation will remove a substantial problem caused by the unavailability of service and parts for the Sigma 3 Computer previously used. The RT11 Multi-System will form the basis for the new on-line program. Preliminary software work has already begun and a target date of December 1, 1978, has been set for the first working version of the program.

### Beam

The beam necessary to do this experiment requires either the Quadrupole Triplet or N30 Dichromatic Target Trains. Tuneup and low intensity running can be accomplished parasitically with any of the present Neutrino train loads. We hope to do a checkout run parasitically, during the Spring run of E-356 with a small amount of beam on the dichromatic target during slow spill by using the vernier steering magnet at the end of the N30 train.

### Staffing and Timing

The proposers listed intend to make this experiment their principal research effort in 1978-79. We have the necessary manpower and expertise to execute the experiment as proposed. Virtually all of equipment exists

or is presently being constructed. We believe the experiment is a useful and exciting extension of the pioneering work done in E-369. We will be ready to start debugging and testing by March 1979 and prepared to execute a high intensity run in the summer. We hope that we can receive approval and begin discussing scheduling before January 1979.

TBWK:dla/lis  
9/5/78

References

- 1 T.Kirk, et.al., submitted to Physical Review Letters (See attached Preprint, Appendix E).
- 2 Particle Data Group, Physics Letters, 75B, April 1978.
- 3 L.M.Lederman, J.Cronin, Rapporteur Talks, "Proceedings of \_\_\_\_\_ Conference on Leptons and Photons at High Energies, \_\_\_\_\_"
- 4 S.D.Drell and T.M.Yan, PRL 25, 316 (1970).
- 5 C.E.Carlson and R.Suaya, Phys. Rev. D 14, 3115 (1976); Phys. Rev D 15, 1416 (1977).
- 6 S.D.Ellis, M.B.Einhorn and C.Quigg, PRL 36, 1263 (1976).
- 7 J.H.Cobb, et.al., Physics Letters 72B, 497 (1978).
- 8 J.G.Branson, et.al., PRL 38, 1331 (1977).
- 9 D.Fong et.al., NP B102, 386(1976)
- 10 J.Whitmore, Multiparticle Production in the Fermilab Bubble Chambers, 1976 (update to Phys. Reports 10C, 273(1974)).
- 11 R.Barate, et.al., Preliminary Results on  $\Psi$  Production and Associated Hadrons by Hadron Collisions, paper presented at the XIIIth Rencontre de Moriord, Les Arcs, France, March 1978.
- 12 A.Billoire, Phys. Lett. 76B, 499 (1978).

## APPENDIX A

### Apparatus Acceptance for Dimuons and Trigger Rates

#### I. Trigger Rates:

The dimuon trigger rates have been computed assuming the apparatus geometry shown in Figure A-1. The magnet center is 7.5 m from the target and gives a 2.115 GeV/c transverse (horizontal) momentum kick to the particles. The primary  $\mu$  detector (M2) is 15 m downstream of the magnet and is shielded by 4.5 m of steel. Another  $\mu$  detector (M1) lies closer to the magnet behind only 2 m of steel. The trigger requires two hits in the counter M2 and our trigger rate stems from three sources:

- (1) real prompt  $\mu^+\mu^-$  ( $\rho, \omega, \phi, \psi$ , continuum),
- (2)  $\pi \rightarrow \mu$  decay, and
- (3) hadron punch through into M2.

We have simulated the real  $\mu^+\mu^-$  rate in a Monte Carlo which used the 225 GeV/c  $\pi^-$ -Carbon data of Branson et al.<sup>8</sup> We generated events according to the form

$$E \frac{dN}{dx_F dp_T} \sim (1 - x_F)^A p_T^B e^{-BP_T} \quad (1),$$

where the parameters A and B have been measured as a function of the dimuon mass by the E-331 group.<sup>8</sup> The overall cross section normalization was also taken from Branson et al.<sup>8</sup> The dimuon object generated using equation (1) was allowed to decay isotropically and the two resulting  $\mu$ 's were tracked through our apparatus.

The  $\pi \rightarrow \mu$  decay and hadron punch-through were simulated using 150 GeV/c  $\pi^-p$  data<sup>9</sup> from the Hybrid 30" Bubble Chamber (E154). Our data summary tape from E154 contains 7000 events with all tracks measured and with overall charge balance. These 7000 events correspond to the total inelastic cross section of 21 mb. The events were scaled to 225 GeV/c (in  $p_{||}$  only,  $p_T$  was not changed) and the multiplicity distribution was corrected to 225 GeV/c values using Whitmore's<sup>10</sup>



data compilation. To increase our statistics we used each event 10 times, rotating the event about the z (beam) axis in  $36^\circ$  increments. Since the  $\pi \rightarrow \mu$  decay probability and the punch-through probability are both low (total  $\sim 1-5\%$  for our geometry) we have enhanced these probabilities by a factor of 15 to increase our " $\mu$  statistics".

The  $\mu$  detector M2 has the dimensions 2.4 m (Y) by 7.3 m (X) and is composed of 60 vertical strip scintillation counters which determine the x position of the  $\mu$ . We intend to time these counters (TDC's) relative to the target interaction time and therefore determine the y position of the  $\mu$ . M2 will be used in the "Bow-Tie" shape which we used in E369 (see Figure A-2). By triggering on hits in diagonally opposed quadrants, we select a pure  $+$  - sample (no like signed pairs). The gap between the upper and lower halves of M2 requires each  $\mu$  to have a minimum  $p_T$ ; this serves to eliminate triggers from low mass pairs. In E369 we physically moved the counters to form the Bow-Tie. For the proposed experiment we may do the same or we may use the TDC information to make the Bow-Tie. Using the TDC's will require a pre-trigger calculation in the PDP 11/45 (see Appendix C) and thus has the disadvantage of increasing the dead time -- the advantage of this mode is its flexibility in determining the exact shape of the Bow-Tie.

We have calculated the trigger rates and events yields for this proposal assuming a Bow-Tie with slope = 0.2, i.e. we require for each  $\mu$

$$\left| \frac{y}{x} \right| > 0.2 \text{ in the M2 counter.}$$

This cut is equivalent to  $(P_T)(\sin \phi) > 280 \text{ MeV/c}$  (independent of  $P_\mu$ ), where  $\phi$  is the azimuthal angle of the  $\mu$ . This is the same Bow-Tie slope used in E369 and therefore the main change is in the size of M2 (see Figure A-2). The increased size in x gives us an increased acceptance for low momentum  $\mu$ 's and therefore an increased acceptance at  $X_F = 0$  where most dimuons are produced (see eqn. (1)). Table I in the main text summarizes the trigger rates for E369 and for this proposal. The "B" Geometry corresponds to a slope cut of 0.2.

In Figure A-3 we show the result of varying the Bow-Tie slope cut in our apparatus. Closing down the Bow-Tie gap gives an unacceptably high trigger rate and only a 30% increase in the number of  $\psi$ 's detected.\* Thus our trigger studies to date have succeeded in re-inventing the wheel (Bow-Tie) used in E369.

## II. Apparatus Acceptance for $\psi, \chi, \psi', \dots$

We have used the Monte Carlo developed for the prompt  $\mu^+\mu^-$  trigger rate to calculate our acceptance for <sup>the</sup> $\psi$  and  $\chi$  families. Specifically, we generate events according to equation (1) with  $A = 2$  and  $B = 2$  (see Branson et al.<sup>8</sup>). For overall normalization we have used the results of E369 where we observed  $\sim 160$   $\psi$ 's for  $\sim 4 \times 10^{10}$   $\pi$ 's incident on a target equivalent to 120 cm of  $\text{LH}_2$ .

We assume the following:

### (1) For $\psi'$ Production:

$$\sigma_{\psi'}/\sigma_{\psi} \sim 0.15 \quad (\text{see Barate et al.}^{11})$$

$$\left. \begin{array}{l} \text{B.R. } \psi' \rightarrow \mu^+\mu^- = 0.8\% \\ \text{B.R. } \psi' \rightarrow \psi \pi^+\pi^- = 33\% \\ \text{B.R. } \psi' \rightarrow \psi \pi^0\pi^0 = 17\% \end{array} \right\} \quad \begin{array}{l} \text{from the Particle} \\ \text{Data Table}^2 \end{array}$$

### (2) For $\chi$ Production:

70% of all  $\psi$ 's come from  $\chi$ 's (our measurement<sup>1</sup>)

The  $\chi$  states are produced in the ratio ( this a prediction of gluon fusion models<sup>5</sup>)

$$\chi(3.411) : \chi(3.510) : \chi(3.55) = 15 : 3 : 20$$

$$\left. \begin{array}{l} \text{BR } \chi(3.411) \rightarrow \psi\gamma = 3.3\% \\ \text{BR } \chi(3.510) \rightarrow \psi\gamma = 23.4\% \\ \text{BR } \chi(3.555) \rightarrow \psi\gamma = 16\% \end{array} \right\} \quad \begin{array}{l} \text{from the Particle} \\ \text{Data Tables}^2 \end{array}$$

\* The number of  $\psi$ 's per experiment was calculated assuming a  $10^7 \pi^-$ /pulse beam incident on a 120 cm  $\text{LH}_2$  target and  $3 \times 10^5$  machine pulses.

More Speculatively we assume the following:

(3)  $^1D_2$  ( $\sim 3.88$  GeV) Production

This state has been predicted by Billoire<sup>12</sup>, to have a production cross section  $\sim \sigma_{\psi'}$ . This state cannot be produced in  $e^+e^-$  collisions at the lowest order in QED.

We take

$$\sigma_{^1D_2} \sim \frac{1}{2} \sigma_{\psi'}$$

$$\text{B.R. } ^1D_2 \rightarrow \psi\eta = 4\%$$

$$\text{B.R. } ^1D_2 \rightarrow \psi\pi\pi = 33\%$$

} guesses based  
on the  $\psi'$

(4)  $^3D_2$  ( $\sim 3.88$  GeV) Production

This state has also been predicted by Billoire<sup>12</sup>, but with a production cross section  $\sim \sigma_{\chi}$ . It also cannot be produced in  $e^+e^-$  collisions at the lowest order in QED.

We take

$$\sigma_{^3D_2} \sim \frac{1}{2} \sigma_{\chi}$$

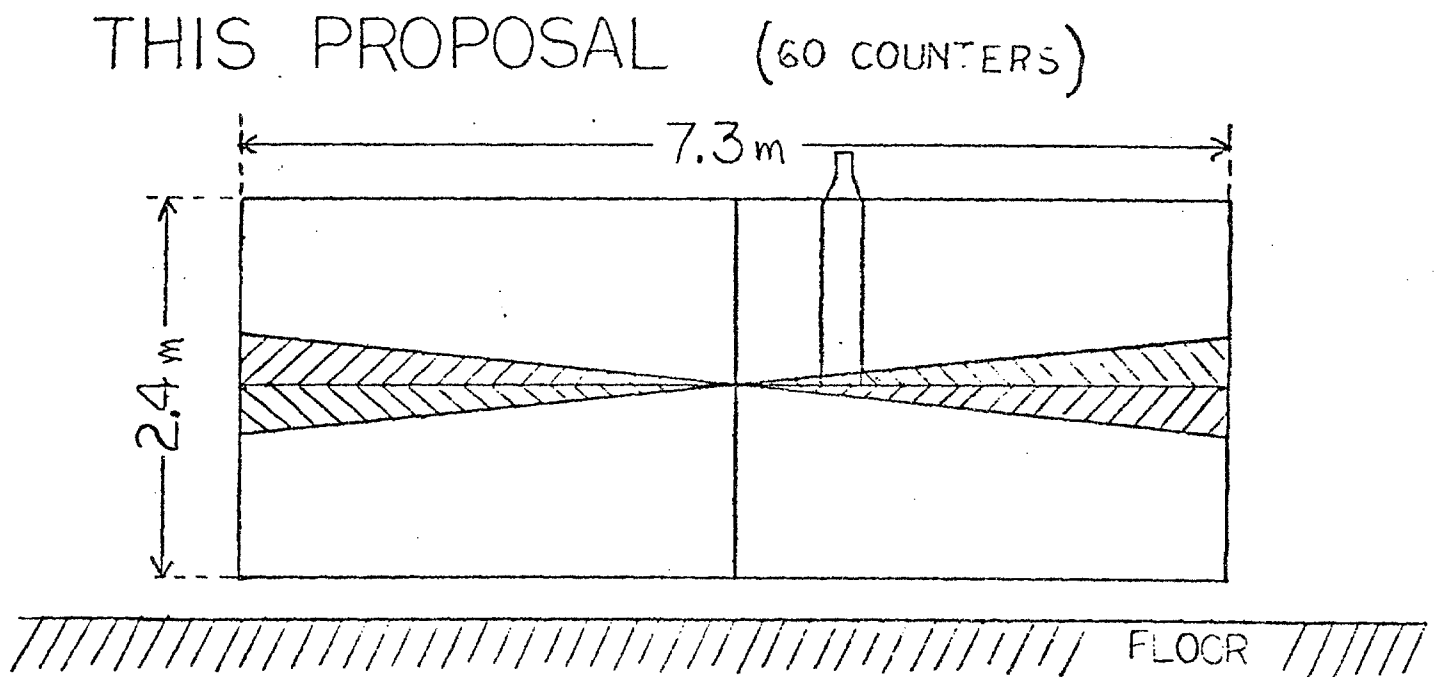
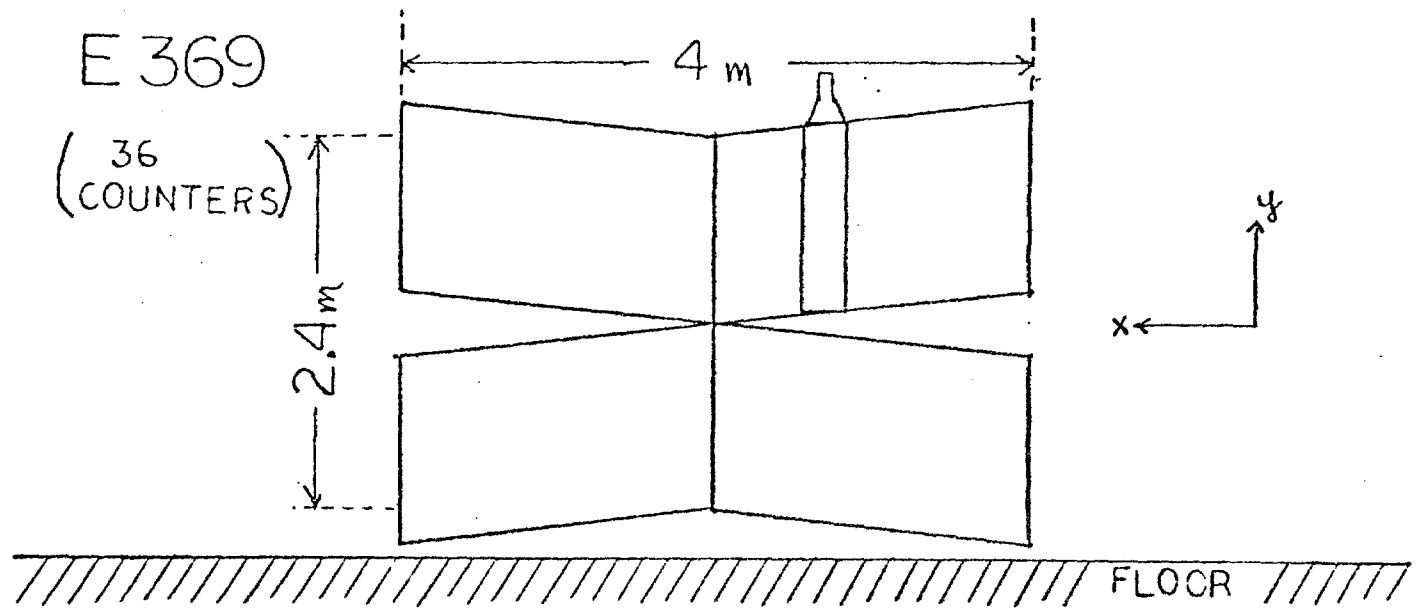
$$\text{B.R. } ^3D_2 \rightarrow \psi\gamma = 10\% \rightarrow \text{based on the } \chi's$$

$$\text{B.R. } ^3D_2 \rightarrow \psi\omega = 10\% \rightarrow \text{a guess}$$

(5)  $\psi D \bar{D}$  Production

The Indiana-Saclay group<sup>11</sup> at CERN has reported 10 such events in the  $K^+\pi^+\pi^+$  decay mode in a sample of 1600  $\psi$ 's. We do not know their acceptance, but assuming it is similar to ours we might expect to see 60 such events in our sample of 10,000  $\psi$ 's.

With the above assumptions we have calculated the yields for  $3 \times 10^{12}$  incident  $\pi$ 's on a 120 cm  $LH_2$  target. The results are in Table A-I.



MUON HODOSCOPE (M2)

FIGURE A-2

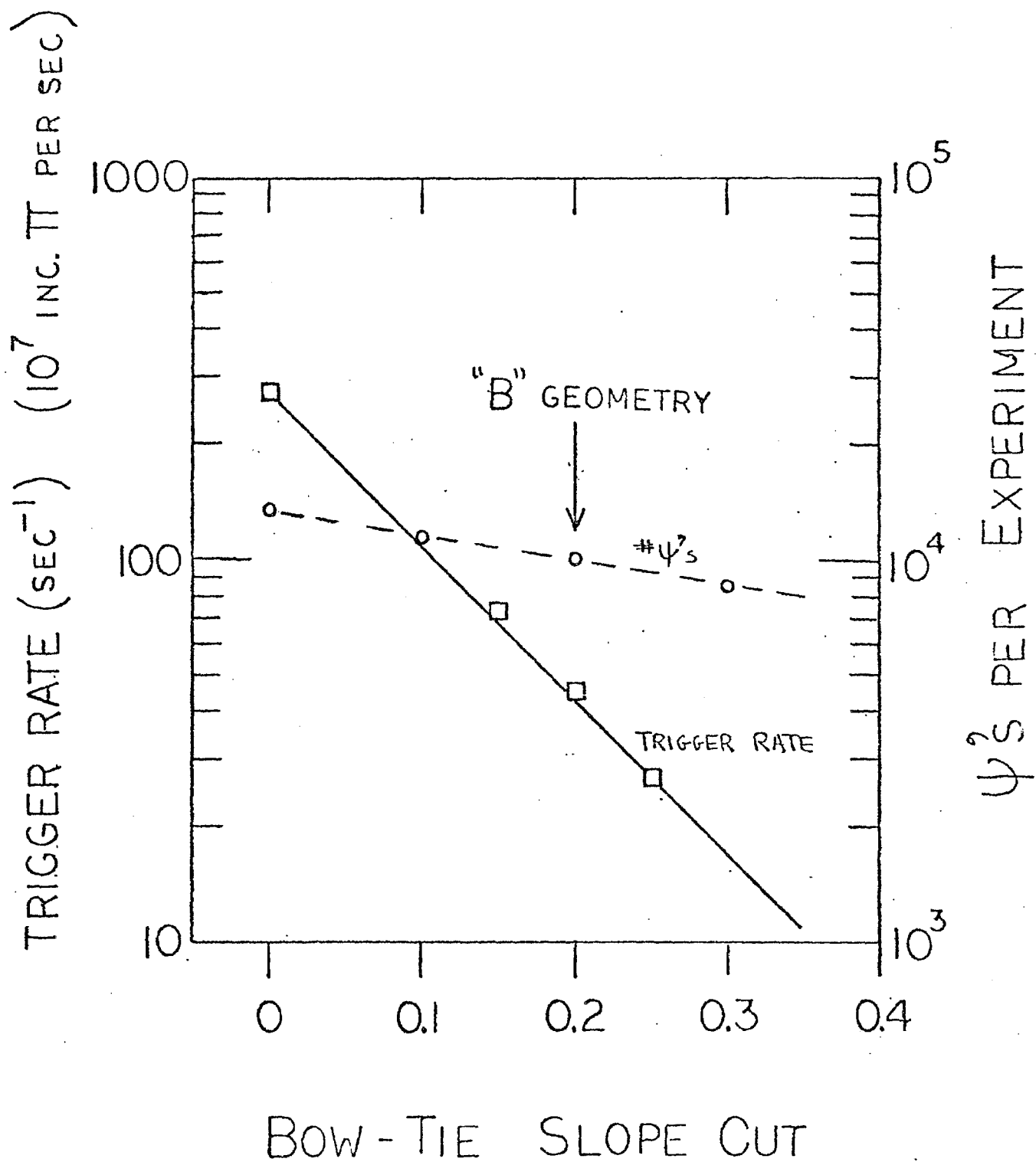


FIGURE A-3

## The Pb Glass Array -- Geometry and Resolution

The new Pb glass array departs from the pure "fly's eye" design of E369 in order to increase solid angle and position resolution without sacrificing energy resolution. As shown in figures B1 and B2, the incoming particles will encounter a double transverse layer of Tufts blocks, a 720 element proportional tube detector for position measurement, and, finally, a fly's eye detector of 47 large University of Illinois blocks.

The Tufts blocks are arranged to give 60 bins over an area 37.5 in. high and 46.0 in. wide, giving excellent position resolution in the vertical (though this measurement is redundant). These two layers constitute a 4.6 radiation length (r.l.) active pre-converter to allow energy measurement beginning at the shower origin.

The 720 element tube detector is shown in greater detail in figure B 3 . It is fabricated of drawn aluminum in cells which are .75 in. wide and .375 in. deep. There are nine layers of roughly 80 elements in each layer--some tilted to resolve ambiguities. This entire stack constitutes .43 r.l. of converter, and will be a small contribution to degradation of the energy resolution. Each element will be pulse height analysed by a system of charge storage units and ADC's. Centroid fitting should allow position resolution of  $\sigma = 5$  mm. in x and y. Similar resolution has been obtained in another experiment with pulse height analysis of a hodoscope array behind 5 r.l. of lead glass.<sup>1</sup>

Energy absorption and measurement is completed in the 47 large rear blocks. Each block is 6 in. X 6 in. X 18 in. (18 r.l.), bringing the total number of radiation lengths to 22.6.

A properly calibrated array will have an energy resolution of  $\sigma = (4\%-6\%) / \sqrt{E}$ . We assume that we can achieve  $\sigma = 5\% / \sqrt{E}$ . The calibration scheme includes one green LED for each block in the array, driven by a common pulser, and a system of optical fiber bundles, driven by a common flash lamp. The LED system has greater long term stability, whereas the optical fiber system has more block-to-block accuracy.

Resolution of individual  $\chi$  states in the mode  $\chi \rightarrow \psi \gamma$  depends critically on the energy and position resolution of the decay photons. For typical values  $E_\psi = 100$  GeV,  $E_\gamma = 10$  GeV:

$$\frac{\partial m_\chi}{\partial \theta} = 16 \frac{\text{MeV}}{\text{mr}}$$

and

$$\frac{\partial m_\chi}{\partial E_\gamma} = 46 \frac{\text{MeV}}{\text{GeV}}$$

Position resolution of  $\sigma = 5$  mm at the 15 m position of the glass array gives an angular resolution of  $\sigma = 1/3$  mr, or

$$\delta m_\chi = 7.4 \text{ MeV from position error.}$$

Energy resolution of  $\sigma = 5\% / \sqrt{E}$  at 10 GeV is  $\sigma = .16$  GeV, yielding

$$\delta m_\chi = 5.3 \text{ MeV from energy determination.}$$

The combined R.M.S. resolution (not including the resolutions on the  $\psi$ ) is then,

$$\delta m_\chi = 9.0 \text{ MeV}$$

This is more than adequate to resolve the  $\chi$  states which are separated by about 40 MeV.

TOP VIEW

FIGURE B1.

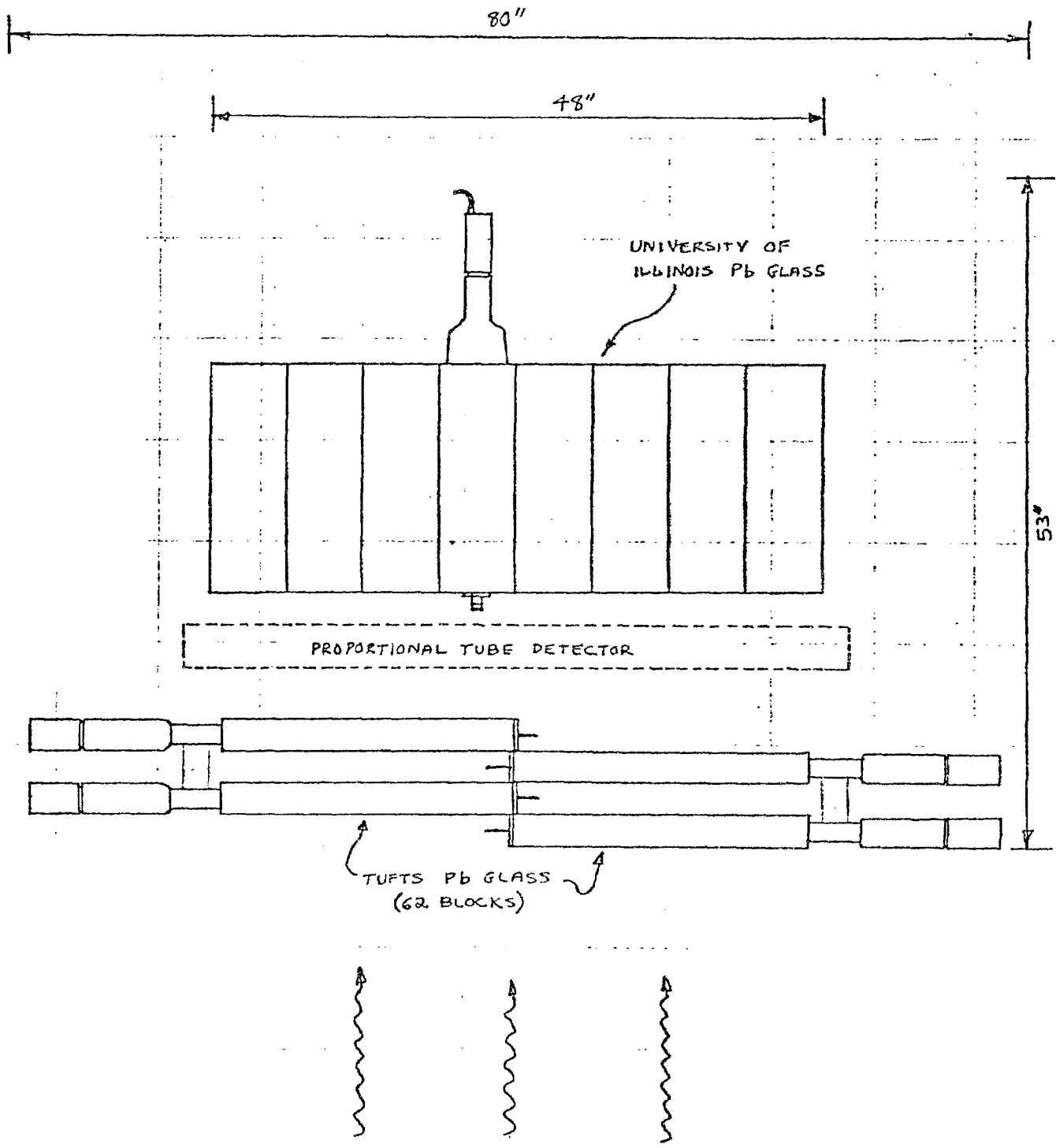




FIGURE B2.

SIDE VIEW

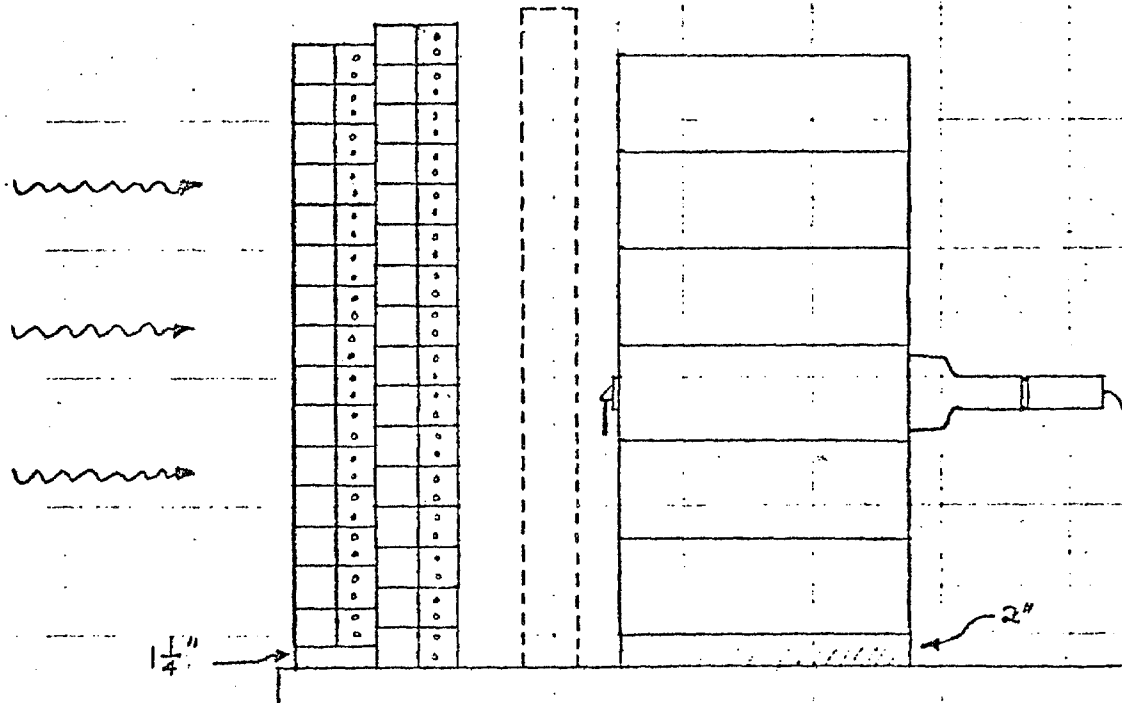
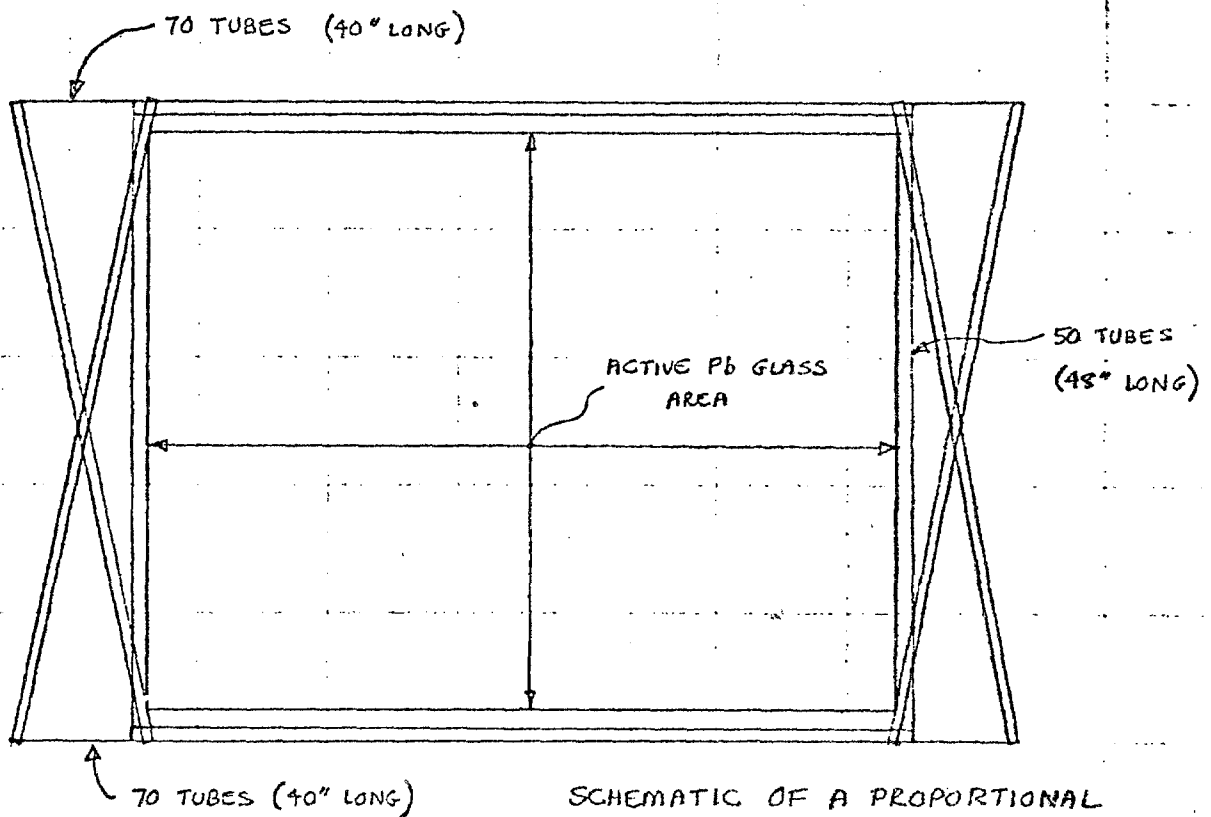


FIGURE B3.

FRONT VIEW



SCHEMATIC OF A PROPORTIONAL  
TUBE TRIPLET. - ONE OF THREE.  
(ONLY END TUBES SHOWN)

## APPENDIX C

### PDP/11 Event Sampling Scheme for Dead Time Suppression

We will implement an "electronic" bow tie arrangement of the muon trigger hodoscope by analysis of the event in the PDP-11, using the following steps:

1. All 60 muon hodoscope elements (which run vertically and resolve the horizontal) will be timed by TDC's, to resolve the vertical.
2. The PDP-11 will begin data acquisition by reading these TDC's (approximately 200 microseconds).
3. The PDP-11 will scan through this list of times, testing each time against a table of allowed time limit values (approximately 300 microseconds).
4. If exactly two elements from opposite quadrants have been hit (about 40 microseconds for this decision), the event readout will proceed. If not, the computer will stop data acquisition of the event and ready the apparatus for the next event (about 10 microseconds).

Trigger sampling will therefore take about 550 microseconds per event, to be compared with a dead time of 6 milliseconds when an event is read in its entirety.

## APPENDIX D

### Multi-Cell Cherenkov Counter:

#### Efficiency and Particle Detection Power

The up-graded 18-cell Cherenkov counter, using dry nitrogen at atmospheric pressure, is expected to provide clear identification of charged K's in the momentum band of approximately 8 GeV/c to 30 GeV/c.

The original Oxford counter has been calibrated by studying the pulse height distributions from fast secondary muons in the summer 1977 E369 run. We find that the distribution in any particular cell is well fitted by an expression involving three cell parameters -- the mean number of photoelectrons per particle,  $\bar{n}$ ; the average gain of the photomultiplier - ADC combination,  $\langle A \rangle$ ; and the standard deviation of the gain,  $\sigma_A$ . Values of these parameters are in the ranges

$\bar{n}(\beta = 1)$	2.8 - 3.8
$\langle A \rangle$	25 - 45 channels per photoelectron
$\sigma_A$	55 - 80% of $\langle A \rangle$

The dependence of  $\bar{n}$  on velocity is known, and has been confirmed for this counter by observation on 12 - 24 GeV/c hadrons selected by the one muon-recoil proton trigger. The observed inefficiencies are consistent with the expected variation of  $\bar{n}$  provided that about 9% of the hadrons are kaons or heavier particles.

For each track belonging to an event we know the momentum and the point of impact in the Cherenkov counter. We can therefore calculate the probability of the set of recorded pulse heights on the hypothesis that all the secondaries are pions,  $\text{Prob}(\pi)$ ; and again on the hypothesis that a track (or tracks) giving a small pulse is a kaon,  $\text{Prob}(K)$ . Since there are approximately ten times as many pions as kaons,  $\text{Prob}(\pi)$  must be much smaller than  $\text{Prob}(K)$  for unambiguous identification of a particle as a kaon. Even when the odds are not overwhelming,

however, one can use a criterion based on the ratio  $\text{Prob}(\pi)/\text{Prob}(K)$  to enrich a sample of probable kaons.

The values of  $\bar{n}(\beta - 1)$  reported above are disappointingly small. They correspond to inefficiencies for fast particles in the range 2-6%. This means typically  $\sim 1/3$  of "identified  $K^{\text{ch}}$ " are misidentified  $\pi$ 's which fail to produce a photoelectron. In order to reduce completely the pion contamination from our kaon sample, we intend to take steps to increase the value of  $\bar{n}(\beta - 1)$  to at least 6 ( $\exp(-6) = 0.2\%$ ). This means only 2-3% of the K's would be misidentified. We shall extend the Cherenkov box by 4 ft., thereby doubling  $\bar{n}$ . No changes will be needed in the mirror or PM tube configuration. The only effect of increasing the gas path is to roughly double the radius of the Cherenkov light circle from its present value of  $\sim 3$  cm. The new radius will still be small compared to the mirror width of about 60 cm., and in any case, algorithms for handling cases of light division between adjacent mirrors will be available.

APPENDIX E

(Submitted to Phys. Rev. Lett.)

$\pi^-$  PRODUCTION OF  $\psi$  AND  $\chi$  PARTICLES AT 217 GeV/c

T. B. W. Kirk and R. Raja

Fermi National Accelerator Laboratory, Batavia, Illinois 60510

and

M. Goodman, W. A. Loomis, A. L. Sessoms, C. Tao, and R. Wilson

Harvard University, Cambridge, Massachusetts 02138

and

G. O. Alverson, G. Ascoli, D. E. Bender, J. W. Cooper, L. E. Holloway,  
L. J. Koester, U. E. Kruse, W. W. MacKay, R. D. Sard, M. A. Shupe,  
and E. B. Smith

The University of Illinois at Urbana-Champaign, Urbana, Illinois 61801

and

J. Davies, T. W. Quirk, and W. S. C. Williams

Department of Nuclear Physics, The University of Oxford,  
Oxford, OX1 3RH, England

and

R. K. Thornton and R. H. Milburn

Tufts University, Medford, Massachusetts 02155

ABSTRACT

Dimuon production is studied in 217 GeV/c  $\pi^-$ -hydrogen and  $\pi^-$ -beryllium collisions in an open geometry with a lead glass array to detect photons associated with the  $\psi$ . The  $\psi$ - $\gamma$  mass spectrum shows a 2.6 standard deviation peak above background at  $\sim 3.5$  GeV. This result implies that  $0.70 \pm 0.28$  of the  $\psi$ 's are produced via the radiative decay of one of the  $\chi(\sim 3.5)$  states.

We have observed production of  $\chi$  ( $\sim 3.5$  GeV) states in an experiment done at Fermilab using a 217 GeV/c  $\pi^-$  beam incident on beryllium and liquid hydrogen targets. It has been suggested<sup>1,2/</sup> that hadronic production of the  $\psi$  occurs primarily through the production of an intermediate  $\chi$  state, followed by the decay  $\chi \rightarrow \psi + \gamma$  or  $\chi \rightarrow \psi + \text{hadrons}$ . A recent result<sup>3/</sup> from the CERN ISR has indicated that such intermediate  $\chi$  states are important in proton-proton collisions. We report here on results obtained in a search for  $\chi \rightarrow \psi + \gamma$  in  $\pi^-N$  interactions.

The Chicago Cyclotron Magnet Spectrometer facility was used in an open geometry to detect and identify particles associated with dimuon production. A schematic drawing of the apparatus is shown in Figure 1. Negative pions of 217 GeV/c strike a 2.5 cm-long beryllium target followed by a 40 cm-long, 3.0 cm-diameter liquid hydrogen target. The trigger required two penetrating particles in diagonally-opposed quadrants of a scintillation counter hodoscope located downstream of a steel hadron absorber (2.5-3.5 m thick). This particular geometric constraint reduced the trigger rate due to prompt low-mass dimuons ( $\rho, \phi$ ) and due to low-mass dimuons originating from pions decaying in flight. During most of the runs, the  $\pi^-$  beam intensity was  $8 \times 10^5$   $\pi$ /pulse. The  $K^-$  and  $\bar{p}$  contaminations of the beam were about 2.5% and 0.5% respectively. The typical trigger rate was 3 per pulse. This report is based on a total incident beam flux of  $4 \times 10^{10}$  pions.

Charged particle positions were measured upstream of the magnet by a 7500 wire system of multiwire proportional chambers and downstream of the magnet by 14 gaps (28 planes) of multiwire spark chambers. The magnet was run with a 14-kG central field. A 2 m-long 18 cell threshold Cherenkov counter

allowed partial  $\pi$ -K separation in an 8-30 GeV/c momentum interval. A 76-element lead-glass Cherenkov array (each 6.35 cm x 6.35 cm x 61 cm, 20.5 radiation lengths) detected photons.

The lead-glass array calibration was monitored during this experiment with an LED system. Following the data run, the array was moved into an electron beam in the Proton area at Fermilab for calibration. To demonstrate the resolution of the lead-glass system, we show in Figure 2 the  $\gamma$ - $\gamma$  mass spectrum for a sample of hadronic triggers from the data run. There is a clear  $\pi^0$  peak with a full width at half maximum of  $\sim 35$  MeV. The  $\eta^0$  is not seen due to the limited transverse acceptance of the array. The background curve in Figure 2 was calculated by pairing  $\gamma$ 's from separate events. All photons are required to have an energy above 5 GeV. Hadronic showers have been removed by a cut on the lateral spread of the shower.

The dimuon mass spectrum above 2.7 GeV is shown in Figure 3. A clear  $\psi$  peak of about 160 events above background is evident. The full width at half maximum of the  $\psi$  peak is 100 MeV and is consistent with the expected resolution of the apparatus. Events with  $\mu^+\mu^-$  effective mass between 2.9 and 3.3 GeV were fit to the one-constraint (1-C) hypothesis that the  $\mu^+\mu^-$  are from the decay of the  $\psi(3098)$ . Demanding a chi-squared less than 10 for the 1-C fits extracts 163  $\psi$  events (referred to hereinafter as 1-C fit  $\psi$ 's); we estimate the non- $\psi$  contamination in these 163 events to be less than 10 events. Figure 4 shows the Feynman  $x$  ( $x_F$ ) and transverse momentum ( $p_T$ ) distributions for the 1-C fit  $\psi$  events. The raw  $x_F$  distribution peaks at 0.45, while the acceptance corrected distribution can be fit to the form  $(1/E)(1-x_F)^A$  with  $A = 1.25 \pm 0.23$ . The  $p_T$  dependence of the  $\psi$  fits the form  $(p_T) \exp(-Bp_T)$  with  $B = 1.45 \pm 0.13$ . We have also fit the  $x_F$  and  $p_T$  distributions separately for  $\pi^-p$  and  $\pi^-Be$  events. The results of these fits are given in Table I.

We have examined the photons associated with the 1-C fit  $\psi$  events. Photons



with (1) energy less than 5 GeV, (2) lateral shower distribution consistent with a hadronic shower, or (3)  $\gamma$ - $\gamma$  invariant mass consistent with the  $\pi^0$  were removed. The cut (1) removes photons in an energy range where our shower finding algorithm is uncertain, but does not remove any  $\chi$  signal (photons from  $\chi$ 's must have  $E_\gamma > 10$  GeV in our apparatus). The cut (2) on lateral shower distributions removes  $\sim 70\%$  of hadronic showers and only  $\sim 15\%$  of real photon showers. Figure 5(a) shows the  $\psi$ - $\gamma$  invariant mass spectrum. The estimated background (dashed line in Figure 5(a)) was obtained by taking photons from events with  $\mu^+\mu^-$  invariant mass in the range 2.7-2.9 GeV and 3.3-4.0 GeV (Non- $\psi$  events) and combining these photons with the complete sample of 1-C fit  $\psi$ 's. This background was then normalized to the number of photons observed in the Non- $\psi$  events, scaled by the ratio of 1-C fit  $\psi$  events to Non- $\psi$  events. The result of subtracting this background is shown in Figure 5(b).

Figure 5 shows a clear peak in the  $\psi$ - $\gamma$  mass spectrum at  $\sim 3.5$  GeV. We fit the distribution in Figure 5(a) with a Gaussian plus the normalized background and find an excess of  $17.2 \pm 6.6$  events centered at 3.51 GeV with a  $\sigma$  of 75 MeV. The confidence level of this fit<sup>4/</sup> is 99%. We expect a  $\psi$ - $\gamma$  mass resolution with  $\sigma \sim 60$  MeV based on the observed width of our  $\pi^0$  peak (see Figure 2) since the error is primarily in the photon energy determination.

If we attribute the excess events at 3.5 GeV to the process  $\chi \rightarrow \psi\gamma$ , we obtain, with a Monte Carlo<sup>5/</sup> determined acceptance of 0.15,

$$\left. \frac{(B_{\chi \rightarrow \psi\gamma})(\sigma_\chi)}{\sigma_\psi} \right|_{x_F \sim 0.5} = 0.70 \pm 0.28.$$

This result compares favorably with the value of  $0.43 \pm 0.21$  obtained by Cobb et al.<sup>3/</sup> at  $x_F \sim 0$  in pp collisions at  $\sqrt{s} = 55$  GeV.

Our  $\sigma \sim 60$  MeV  $\psi$ - $\gamma$  mass resolution does not allow us to clearly separate the  $\chi(3415)$ :  $\chi(3510)$ :  $\chi(3555)$  states, although our fit indicates the higher mass is preferred. We note that a current gluon fusion model<sup>1/</sup> predicts production cross sections for these states in the ratio 3:4 for  $\chi(3415)$ :  $\chi(3555)$ . Production of the  $\chi(3510)$  by fusion of two gluons is forbidden. Folding in the measured<sup>6/</sup> branching ratios for  $\chi \rightarrow \psi\gamma$ , we would expect to see  $\psi$ - $\gamma$ 's in the ratio 1:6.5 for  $\chi(3415)$ :  $\chi(3555)$ . Our data is consistent with this ratio.

To recapitulate, our measurement of the  $\psi$ - $\gamma$  mass spectrum in the region 3.4-3.6 reveals an excess of  $17.2 \pm 6.6$  events above the expected background. Including acceptance corrections, this result implies that  $\sim 70\%$  of all  $\psi$ 's in  $\pi^-N$  interactions at 217 GeV/c near  $x_F = 0.5$  come from the production of  $\chi$  states followed by the decay  $\chi \rightarrow \psi\gamma$ .

We would like to thank the staff of the Fermilab Neutrino and Proton Areas for their help in this experiment and the members of the CHIO Muon Collaboration for the loan of equipment built by them. We also thank the University of Chicago for the loan of their Sigma-3 on-line computer and particularly S. C. Wright for his help with the Sigma-3. Mr. Stephen Hahn was instrumental in the data reduction at the University of Illinois. This work was supported by the U. S. Department of Energy under contracts EY-76-C-02-3000, EY-76-C-02-3064, EY-76-C-02-1195, EY-76-C-02-3023, and by the Science Research Council (United Kingdom).

Figure Captions

- Fig. 1. The Chicago Cyclotron Magnet Spectrometer Facility as configured for this experiment.
- Fig. 2. The  $\gamma$ - $\gamma$  mass spectrum for a sample of hadronic triggers. The curve is a background calculated using uncorrelated  $\gamma$ 's and is normalized to the number of events in the mass range 0.25-0.50 GeV.
- Fig. 3. The  $\mu^+\mu^-$  invariant mass spectrum.
- Fig. 4. (a) The  $x_F$  distribution for the one-constraint  $\psi$  event fits. The solid histogram indicates the raw data distribution and the open circles are the acceptance-corrected points. The dashed curve is a fit to the form  $dN/dx_F \sim (1/E)(1-x_F)^{1.25}$  (see text).  
(b) The acceptance-corrected distribution  $(1/p_T) dN/dp_T$  for the one-constraint  $\psi$  event fits. The curve is a fit to the form  $\exp(-1.45 p_T)$  (see text).
- Fig. 5. (a) The  $\psi$ - $\gamma$  invariant mass spectrum. The dashed curve is the estimated background (see text). The error bar on the background curve reflects the uncertainty in our normalization.  
(b) The  $\psi$ - $\gamma$  invariant mass spectrum after subtraction of the background shown in (a).

Table A-I.  $\psi, \chi, \psi', \dots$  Acceptances and Yields

	E-369		THIS PROPOSAL	
	% acceptance	# events	% acceptance	# events
$\psi \rightarrow \mu^+ \mu^-$	9.8	160	10.8	10,000
$\chi(3.41) \rightarrow \psi \gamma$	1.9	2.5	5.2	380
$\chi(3.51) \rightarrow \psi \gamma$	1.7	3.3	5.1	530
$\chi(3.55) \rightarrow \psi \gamma$	1.7	14.5	5.1	2,400
$\psi' \rightarrow \mu^+ \mu^-$	8.9	2.5	10.6	170
$\psi' \rightarrow \psi \pi^+ \pi^-$	7.0	5.8	7.3	330
$^1D_2 \rightarrow \psi \gamma$	0.5	1.2	3.0	430
$^1D_2 \rightarrow \psi \omega$	1.0	2.4	3.4	45
$^3D_2 \rightarrow \psi \eta$	2.4	0.05	2.6	3
$^3D_2 \rightarrow \psi \pi^+ \pi^-$	5.2	2	6.6	150
$\psi \xrightarrow{DD} K^\pm \pi^\mp \pi^\mp$ $\downarrow$ $\mu^+ \mu^-$	2.2	1	2.9	60

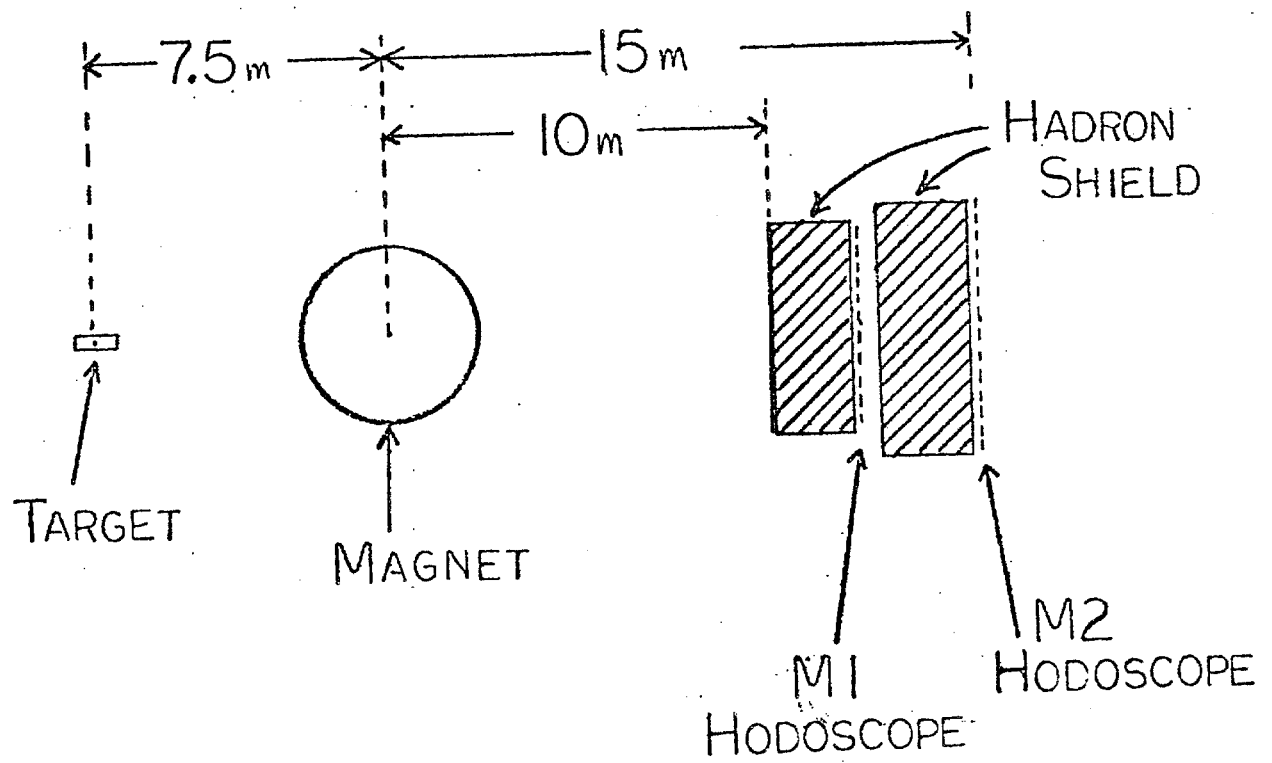


FIGURE A-1

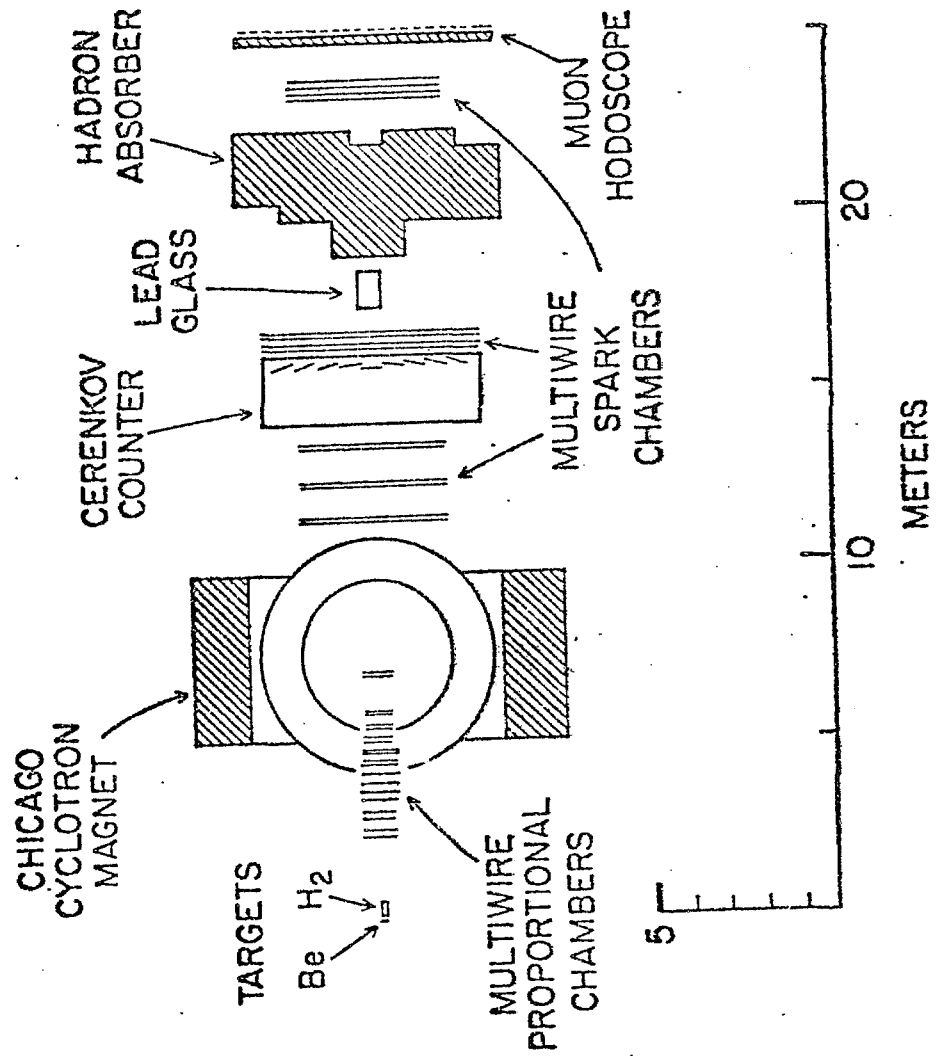


Figure 1

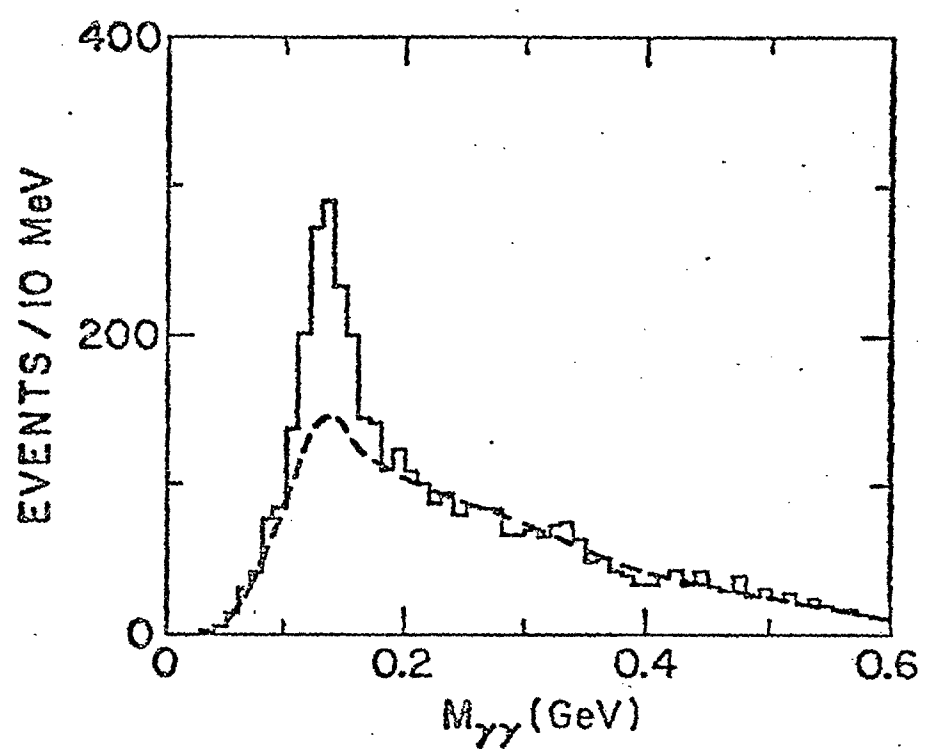


Figure 2

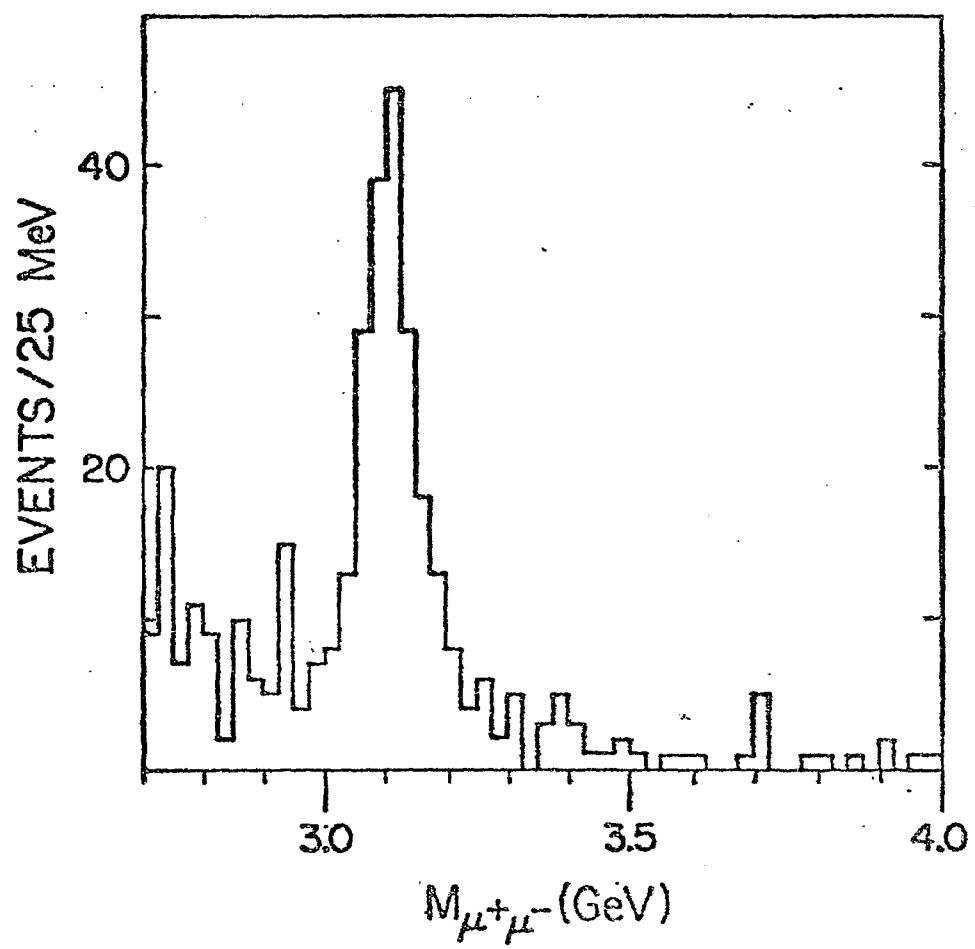


Figure 3



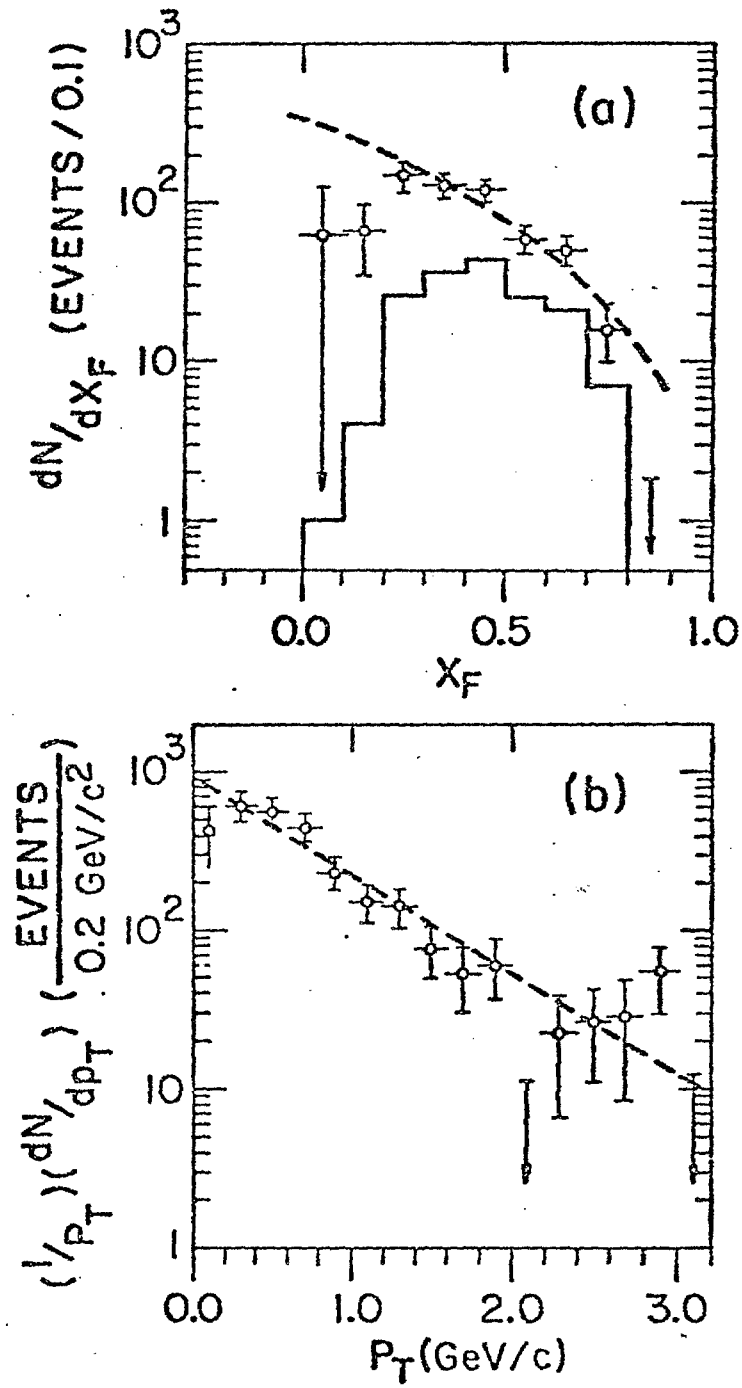


Figure 4

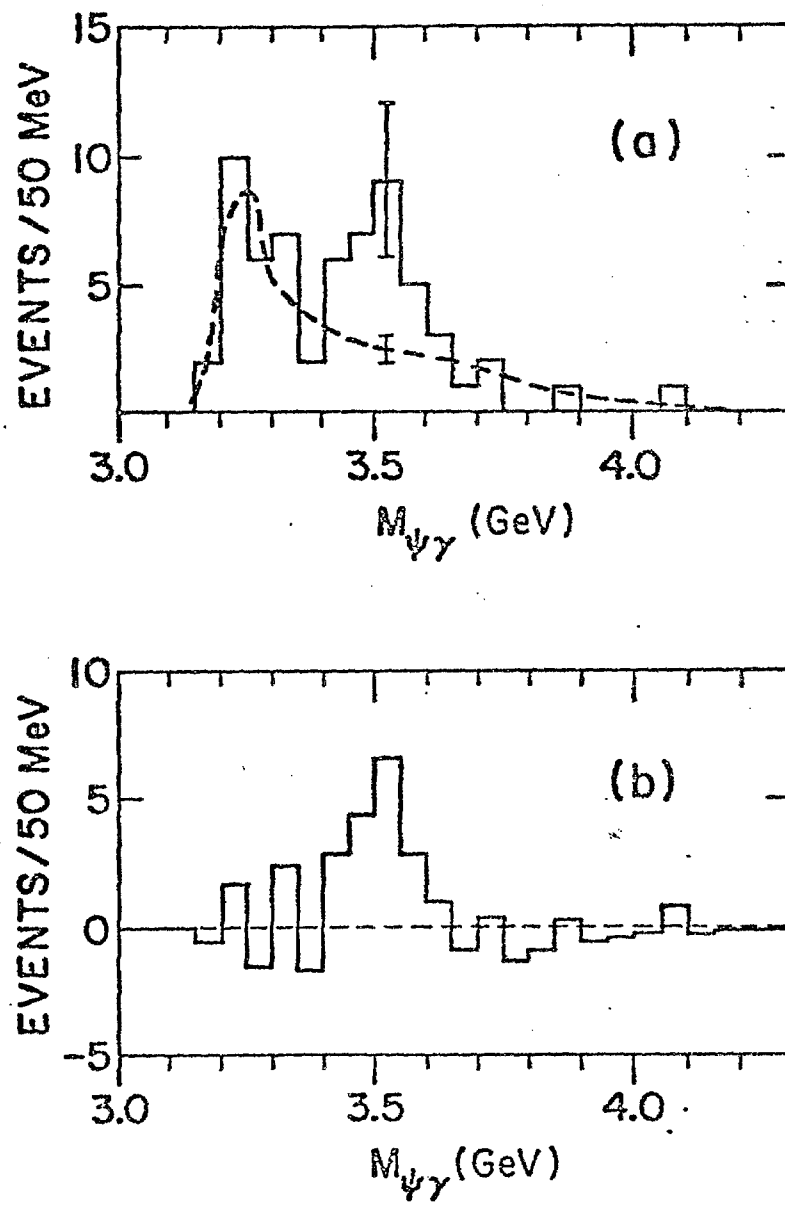


Figure 5

TABLE I. Results of  $\psi$  invariant cross section fits for acceptance-corrected distributions in  $x_F$  and  $p_T$ .  $(E)(dN/dx_F)$  was fit to the form  $(1 - x_F)^A$  in the  $x_F$  range 0.1-0.9.  $(E/p_T)(dN/dp_T)$  was fit to the form  $\exp(-Bp_T)$  in the  $p_T$  range 0.0-3.2 GeV/c.

Interaction	A	Confidence Level	B(GeV/c <sup>-1</sup> )	Confidence Level
$\pi^- p$ and $\pi^- Be$	$1.25 \pm 0.23$	0.013	$1.45 \pm 0.13$	0.19
$\pi^- p$	$1.11 \pm 0.28$	0.24	$1.16 \pm 0.18$	0.18
$\pi^- Be$	$1.39 \pm 0.33$	0.41	$1.66 \pm 0.22$	0.86
$\pi^- C^a$	$1.93 \pm 0.20$	---	$1.98 \pm 0.13$	---
$\pi^+ C^a$	$1.33 \pm 0.21$	---	$2.06 \pm 0.10$	---

<sup>a</sup> These results are from Reference 7.

REFERENCES

1. C. W. Carlson and R. Suaya, Phys. Rev. D14, 3115 (1976), and Phys. Rev. D15, 1416 (1977), and Hadronic Production of Heavy-Quark Bound States, to be published in Phys. Rev. D, 1 August 1978.
2. S. D. Ellis, M. B. Einhorn and C. Quigg, Phys. Rev. Lett. 36, 1263 (1976).
3. J. H. Cobb et al., Phys. Lett. 72B, 497 (1978).
4. The confidence level of a fit to the data in Figure 5(a) by the background curve alone (no signal) is 12%.
5. The Monte Carlo calculation assumed  $\chi(\sim 3.5)$  production according to  $(d^2N/dx_F dp_T) \sim (1-x)^2 p_T \exp(-2 p_T)$  and an isotropic decay of  $\chi \rightarrow \psi\gamma$ .
6. Particle Data Group, Phys. Lett. 75B (1978).
7. J. G. Branson et al., Phys. Rev. Lett. 38, 1331 (1977).